

INFLUENCE OF AL ADDITION ON THE THERMAL STABILITY AND MECHANICAL PROPERTIES OF $\text{Fe}_{76.5-x}\text{Cu}_1\text{Si}_{13.5}\text{B}_9\text{Al}_x$ AMORPHOUS ALLOYS

Y.Y. Sun, M. Song #

State Key Laboratory of Powder Metallurgy, Central South University,
Changsha 410083, China

(Received 27 July 2011; accepted 31 August 2011)

Abstract

This paper fabricated $\text{Fe}_{76.5-x}\text{Cu}_1\text{Si}_{13.5}\text{B}_9\text{Al}_x$ ($x=0,1,2,3,5,7$ at.%) amorphous ribbons using single-roller melt-spinning method. The effect of Al content on the thermal stability and mechanical properties was investigated. The results indicated that Al addition have little effect on the amorphous formation ability of the alloys. On the other hand, increasing the Al content can substantially increase T_{x2} , which corresponds to the crystallization of Fe borides. Nanoindentation tests indicated that hardness of the alloys increase slightly with increasing the Al content, and Young's modulus has a complicated relationship with the Al content.

Keywords: Fe-Cu-Si-B alloy; Nanoindentation; Amorphous; Shear bands

1. Introduction

Fe is one of the most widely used components in magnetic materials. Due to the rapid development in some fields, such as electronic communication, automation and recording media, extensive attentions have been paid to Fe-based alloys [1,2]. The family of Fe-Cu-Nb-Si-B alloys (also called

Finemet alloys) is a kind of excellent soft magnetic materials and have widely been used in industrial applications [3,4]. This type of the alloys is typically produced from amorphous precursors that are partially devitrified, resulting in nano-scaled ferromagnetic grains embedded in the residual amorphous matrix. However, the price of producing Finemet alloys is very

Corresponding author: min.song.th05@alum.dartmouth.org

high due to the high cost of the Nb element. Thus, the Nb-free soft magnetic alloys have been developed, such as Fe-Cu-B, Fe-Cu-Si-B (Ohta, 2007) [5-7] nanocrystalline soft magnetic alloys with improved saturation magnetization (M_s) as high as 1.8 T, for the economical and practical considerations. At the same time, substitution of Nb by other cheap elements is another effective way to cut the cost. Previous works showed that the substitution of Nb by Al element, with the similar atom radius (0.143 nm) to Nb, in Finemet alloys has a great effect on the magnetic properties, such as increasing the saturation magnetization (M_s) [8-10], decreasing the coercivity (H_c) [9-13], enhancing the Curie temperature when the Al content is up to 3 at.% [14] and decreasing the magnetocrystalline anisotropy K_1 [9,15]. However, almost all the investigations concentrated on the magnetic properties of the Fe-Cu-Si-B-Al alloys, and not much information exists on the effects of the Al addition on the structures and the corresponding mechanical properties. Therefore, in this work, the effects of Al addition on the mechanical properties of Nb-free Fe-Cu-Si-B amorphous alloys were studied using X-ray diffractometer (XRD), transmission electron microscope (TEM), differential scanning calorimetry (DSC) and nanoindentation technique.

2. Experimental

Master alloy ingots with the nominal composition of $\text{Fe}_{76.5-x}\text{Cu}_1\text{Si}_{13.5}\text{B}_9\text{Al}_x$ ($x=0, 1, 2, 3, 5, 7$, atomic percentage) were prepared by arc melting high-purity Fe (99.9%), B (99.9%), Si (99.9%), Al (99.9%)

and Cu (99.9%) in a Ti-gettered high-purity argon atmosphere. The ingots were re-melted five times and stirred by a magnetic beater to ensure its compositional homogeneity. Melt-spun ribbons with 20 μm in thickness and 1.5 mm in width were prepared by single-roller melt-spinning method under an argon atmosphere with a speed of about 50 m/s. The fabricated ribbons were very flexible and could be bent by 180° without cracking.

The microstructures of the ribbons were studied using a Dmax 2500VB X-ray diffractometer (XRD) with Cu-K α radiation and a JEOL 3000F field emission transmission electron microscope (TEM). Crystallization kinetics of the alloys was investigated by differential scanning calorimetry (DSC, NETZSCH STA 449C) with a scanning rate of 0.33 K/s. Mechanical properties were studied using an Ultra Nanoindentation tester (CSM) with the maximum loads as high as 10 mN. The loading and unloading procedures were carried out under a load control of 20 mN per minute, with the dwell period of 15 seconds being imposed before unloading. Berkovich tip was impressed into the longitudinal cross section of the ribbons, which were mechanically polished with 1/4 μm and 1 μm diamond abrasives firstly. At least 10 tests were performed on each sample to obtain enough statistical significance on the hardness and Young's modulus.

3. Results and Discussion

3.1. X-ray diffraction and microstructures

Figure 1 shows the XRD patterns of the fabricated $\text{Fe}_{76.5-x}\text{Cu}_1\text{Si}_{13.5}\text{B}_9\text{Al}_x$ ribbons

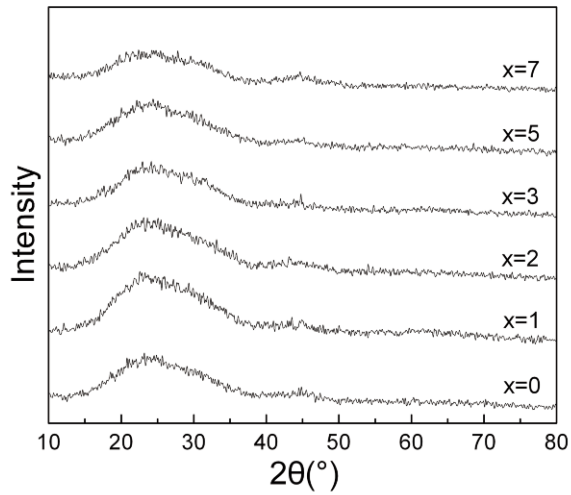


Figure 1: XRD patterns of the $Fe_{76.5-x}Cu_1Si_{13.5}B_9Al_x$ ribbons.

with $x = 0\sim 7$ at.%. The patterns consist of broad halos without obvious detectable peaks, indicating the presence of a single amorphous phase within the detection limit of XRD.

Figure 2(a) and the inset show a bright-field image and the corresponding selected area diffraction (SAED) pattern of the $Fe_{75.5}Cu_1Si_{13.5}B_9Al_1$ ($x=1$) ribbon. The absence of contrast in the bright-field image and a broad diffuse halo in the SAED pattern indicate the formation of a completely amorphous structure. The high-resolution transmission electron microscope (HRTEM) image in Figure 2(b) can further confirm the amorphous structure due to the disorder lattice arrangement. It should be noted that similar features were also observed for the rest alloy ribbons ($x = 0\sim 7$ at.%). This indicates that all the alloys with different Al contents have good amorphous formation ability.

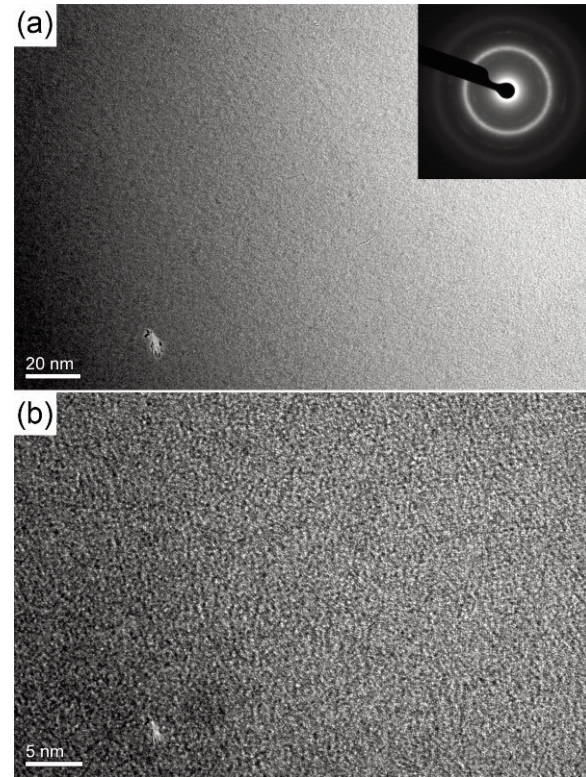


Figure 2: (a) Bright-field TEM image and the corresponding SAED patterns of the melt-spun $Fe_{75.5}Cu_1Si_{13.5}B_9Al_1$ ribbon and (b) HRTEM image.

3.2. DSC curves

Figure 3 shows typical DSC curves of the $Fe_{76.5-x}Cu_1Si_{13.5}B_9Al_x$ ribbons with a heating rate of 0.33 K/s and the relationship between T_{x1} and T_{x2} and Al content. It can be seen from Figure 3a that all the amorphous ribbons did not show an obvious glass transition before crystallization, indicating that the $Fe_{76.5-x}Cu_1Si_{13.5}B_9Al_x$ ribbons are not glassy but ordinary amorphous alloys [16].

Two distinct exothermic peaks on the

curves indicate that the crystallization of all studied ribbons is through a two-step process. It should be noted that the first crystallization peak corresponds to the formation of α -Fe(Si) phase, and the second one corresponds to the formation of Fe

borides, according to the previous investigations [17,18]. It should also be noted that the onset temperature T_{x1} of the first crystallization process remains almost constant (around 734 K within the detection limit of the DSC), while the onset temperature T_{x2} of the second crystallization process increase dramatically with increasing the Al content. This phenomenon indicates that Al addition has little effect on the amorphous formation ability and/or the formation of crystalline α -Fe(Si) phase due to the relatively stable T_{x1} with increasing the Al content. On the other hand, the increased T_{x2} with increasing the Al content was also observed in Fe-Al-B ternary amorphous alloys, in which the crystallization temperature corresponding to the formation of Fe borides increases with increasing the Al content [19]. It is well known that crystallization of amorphous alloys is a nucleation/growth process, which is dominated by the diffusion of base metals. It can thus be concluded from Figure 3 that the addition of Al might substantially inhibit the diffusion of B instead of Fe, since the formation temperature of single phase α -Fe(Si) remains constant, while that of the Fe borides increases dramatically with increasing the Al content.

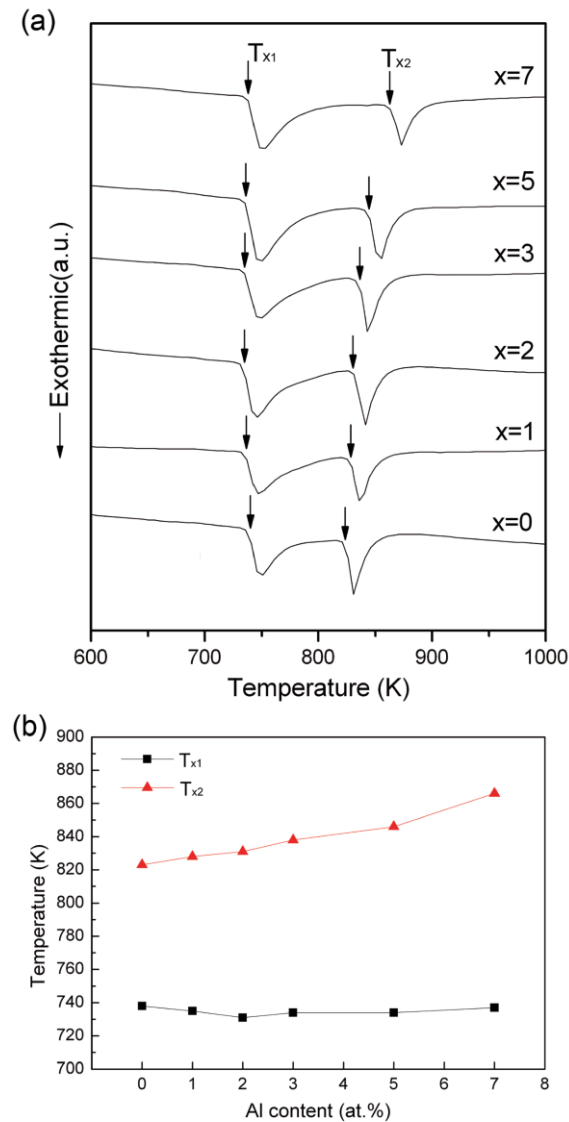


Figure 3: (a) DSC curves of the $Fe_{76.5-x}Cu_1Si_{13.5}B_9Al_x$ ribbons with a scanning rate of 0.33K/s and (b) the relationship between T_{x1} and T_{x2} and Al content.

3.3. Mechanical properties

Figure 4a shows the typical load-displacement (P-h) curves of specimens with different Al contents under a load of 10 mN. It can be seen from Figure 4a that the loading parts of all the curves are relatively smooth without obvious pop-in events, differing from many other amorphous systems such as

Zr-based, Pd-based and Mg-based metallic glasses [20,21]. Wright et al. [22,23] concluded that each pop-in corresponds to the operation of a single shear band that quickly accommodates the applied strain in BMG, and larger pop-in displacement corresponds to greater shear displacements within the shear band. A previous study [24] indicated that the absence of pop-in during nanoindentation for Fe-Cu-Si-B amorphous alloys might be due to the small size of shear bands (less than 1 μm), and the simultaneous operation of the multiple shear bands.

Figure 4b shows the dependence of the Young's modulus and hardness obtained during nanoindentation as a function of Al content. It can be seen from Figure 4b that the evolution of the Young's modulus with Al content is very complicated. The Young's modulus has the maximum value of 164.8 GPa and minimum value of 122.5 GPa when $x=0$ and $x=2$, respectively. It is widely accepted that Young's modulus is one of the fundamental elastic properties representing the interatomic distance and bonding strength between atoms [25]. The evolution of Young's modulus with Al content indicates that Al atom has a relative complex effect on the bonding strength in Fe-Cu-Si-B alloys.

It can also be seen from Figure 4b that increasing the Al content can slightly improve the hardness from ~ 9 GPa to ~ 9.6 GPa when the Al content increases from 0% to 7 at.%, except for the specimen with 2 at.% Al addition, which has an abnormal high hardness. It is known that the plastic deformation of amorphous alloys is through the nucleation and propagation of the shear bands [26]. These microscopic shear bands

generated during nanoindentation can be observed using atom force microscope (AFM).

Figure 5 shows a typical AFM image of the $\text{Fe}_{75.5}\text{Cu}_1\text{Si}_{13.5}\text{B}_9\text{Al}_1$ ribbon after nanoindentation. It can be seen from Figure 5 that semi-circle patterns around indented hole are observed (arrowed in Figure 5) and correspond to the shear bands, which are nucleated outside of the indents when the indenter moves deeper into the sample, and pile up as the material flow upwards and away from the depth of the indents. The

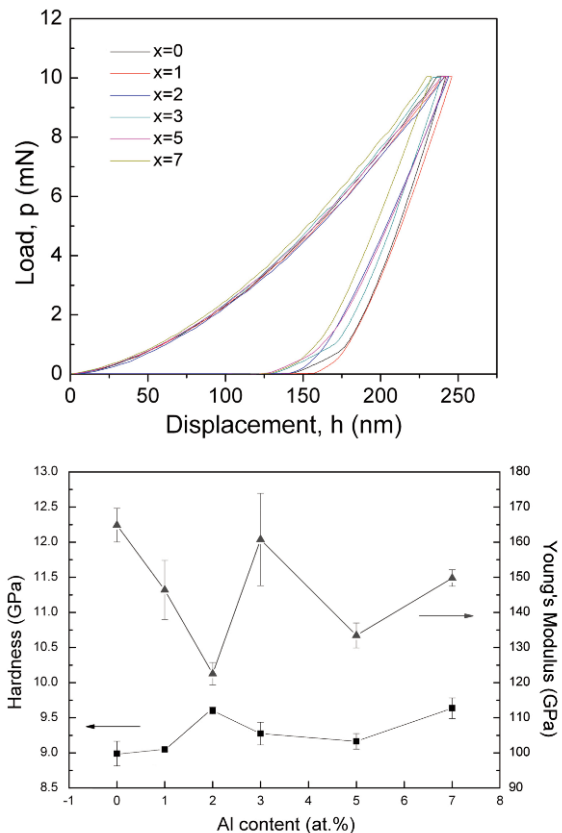


Figure 4: (a) load-displacement curves of Fe-Cu-Si-B-Al alloy and (b) the relationship between hardness and Young's modulus and Al content.

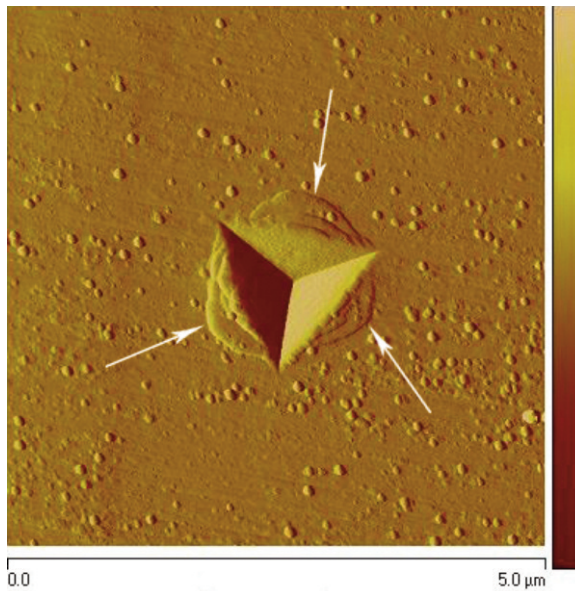


Figure 5: An AFM image of the indented pattern of $Fe_{75.5}Cu_1Si_{13.5}B_9Al_1$ ribbon under a load of 10 mN.

semi-circle patterns were observed for all the specimens with different Al contents. It can be seen that the semi-circle patterns around each side of indented hole are almost symmetrical, resulting from the simultaneous nucleation and propagation of several shear bands under the sharp Berkovich indenter during nanoindentation. Wright et al. pointed out that each pop-in event (sudden displacement excursion) occurred on load-displacement curve corresponds to the operation of a single shear band [22,23]. Due to the simultaneous operation of shear bands, the load-displacement curves of all studied amorphous alloys appear relatively smooth, as shown in Figure 4a, and no obvious pop-in was detected. The similar result was also observed in Fe-Cu-Si-B bulk metallic glass during nanoindentation [24].

4. Conclusion

In this work, $Fe_{76.5-x}Cu_1Si_{13.5}B_9Al_x$ ($x=0,1,2,3,5,7$ at.%) amorphous ribbons were prepared by single-roller melt-spinning method and the effect of Al content on the thermal stability and mechanical properties was investigated. The results indicated that Al addition have little effect on improving the amorphous formation ability. However, increasing the Al content can increase T_{x2} , which corresponds to the crystallization of Fe borides. The hardness of $Fe_{76.5-x}Cu_1Si_{13.5}B_9Al_x$ alloys increase slightly with increasing the Al content.

Acknowledgements

This work is financially supported by Hunan Provincial Natural Science Foundation of China (11JJ2024), the Program for New Century Excellent Talents in University (NCET-10-0842) and Fundamental Research Funds for the Central Universities (2011JQ021).

References

- [1] A. Grujić, N. Talijan, D. Stojanović, J.S. Trošić, Z. Burzić, L.j. Balanović, R. Aleksić, J. Min. Metall. Sect. B, 46 B (2010) 25.
- [2] N. Talijan, V. Čosović, T. Žák, A. Grujić, J. Stajic-Trošić, J. Min. Metall. Sect. B, 45 (2009) 111.
- [3] Y. Yoshizawa, S. Oguma, K. Yamauchi, J. Appl. Phys. 64 (1988) 6044.
- [4] J. Petaold, J. Magn. Mat. 242-245 (2002) 84.
- [5] M. Ohta, Y. Yoshizawa, Jpn J. Appl. Phys 46

- (2007) L477.
- [6] M. Ohta, Y. Yoshizawa, *Mater. Trans.* 48 (2007) 2378.
- [7] M. Ohta, Y. Yoshizawa, *Appl. Phys. Lett.* 91 (2007) 2062517-1.
- [8] P.J. Warren, I. Todd, H.A. Davies, A. Cerezo, M.R.J. Gibbs, D. Kendall, R.V. Major, *Scr. Mater.* 41 (1999) 1223.
- [9] B.J. Tate, B.S. Parmar, I. Todd, H.A. Davies, M.R.J. Gibbs, R.V. Major, *J. Appl. Phys.* 83 (1998) 6335.
- [10] B.S. Dong, S.X. Zhou, M.J. Hu, W.Z. Chen, B.L. Shen, *Mater. Lett.* 64 (2010) 736.
- [11] I. Todd, B.J. Tate, H.A. Davies, M.R.J. Gibbs, D. Kendall, R.V. Major, *J. Magn. Magn. Mater.* 215-216 (2000) 272.
- [12] Z.J. Yan, B.R. Bian, Y. Hu, S.E. Dang, L.T. Xia, Y.M. Wang. *J. Magn. Magn. Mater.* 322 (2010) 3359.
- [13] M. Daniil, M.S. Osofsky, D.U. Gubser, M.A. Willard, *Appl. Phys. Lett.* 96 (2010) 162504.
- [14] A. Zorkovska, J. Kovac, P. Sovak, P. Petrovic, M. Konc, *J. Magn. Magn. Mater.* 215-216 (2000) 492.
- [15] S.H. Lim, W.K. Pi, T.H. Noh, H.J. Kim, I.K. Kang, *J. Appl. Phys.* 73 (1993) 6591.
- [16] T. Bitoh, A. Makino, A. Inoue, *J. Appl. Phys.* 99 (2006) 08F102.
- [17] T.H. Noh, M.B. Lee, H.J. Kim, I.K. Kang. *J. Appl. Phys.* 67 (1990) 5568.
- [18] Y. Yoshizawa, K. Yamauchi, *Mater. Sci. Eng. A* 133 (1991) 176.
- [19] A. Inoue, A. Kitamura, T. Masumoto, *J. Mater. Sci.* 16 (1981) 1895.
- [20] C.A. Schuh, A.C. Lund, T.G. Nieh, *Acta. Mater.* 52 (2004) 5879.
- [21] C.A. Schuh, T.G. Nieh, *Acta. Mater.* 51 (2003) 87.
- [22] W.J. Wright, R. Saha, W.D. Nix, *Mater. Trans. JIM* 42 (2001) 642.
- [23] C.A. Pampillo, *J. Mater. Sci.* 10 (1975) 1194.
- [24] Y.Y. Sun, M. Song, X.Z. Liao, Y.H. He, *J. Alloys Comp.* 509 (2011) 6603.
- [25] J.G. Wang, B.W. Choi, T.G. Nieh, C.T. Liu, *J. Mater. Res.* 15 (2000) 798.
- [26] C.A. Pampillo, *J. Mater. Sci.* 10 (1975) 1194.